View metadata, citation and similar papers at core.ac.uk

brought to you by CORE

provided by HKU Scholars Hub

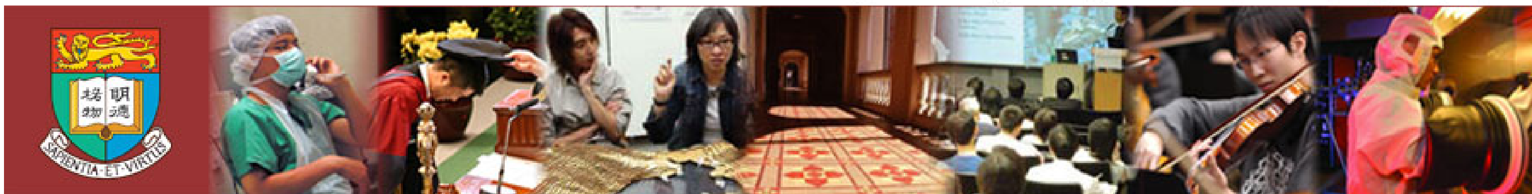

Title	Strain in epitaxial Bi2Se3 grown on GaN and graphene substrates: A reflection high-energy electron diffraction study
Author(s)	LI, B; GUO, X; Ho, WK; Xie, MH
Citation	Applied Physics Letters, 2015, v. 107 n. 8, article no. 081604
Issued Date	2015
URL	http://hdl.handle.net/10722/218819
Rights	Creative Commons: Attribution 3.0 Hong Kong License

Strain in epitaxial Bi_2Se_3 grown on GaN and graphene substrates: A reflection high-energy electron diffraction study

Bin Li, Xin Guo, Wingkin Ho, and Maohai Xie[a)]
Department of Physics, The University of Hong Kong, Pokfulam Road, Hong Kong

(Received 8 June 2015; accepted 16 August 2015; published online 27 August 2015)

Topological insulator (TI) has been one of the focus research themes in condensed matter physics in recent years. Due to the relatively large energy bandgap, Bi_2Se_3 has been identified as one of the most promising three-dimensional TIs with application potentials. Epitaxial Bi_2Se_3 by molecular-beam epitaxy has been reported by many groups using different substrates. A common feature is that Bi_2Se_3 grows readily along the *c*-axis direction irrespective of the type and condition of the substrate. Because of the weak van deer Waals interaction between Bi_2Se_3 quintuple layers, the grown films are reported to be strain-free, taking the lattice constant of the bulk crystal. At the very initial stage of Bi_2Se_3 deposition, however, strain may still exist depending on the substrate. Strain may bring some drastic effects to the properties of the TIs and so achieving strained TIs can be of great fundamental interests as well as practical relevance. In this work, we employ reflection high-energy electron diffraction to follow the lattice constant evolution of Bi_2Se_3 during initial stage depositions on GaN and graphene, two very different substrates. We reveal that epitaxial Bi_2Se_3 is tensile strained on GaN but strain-free on graphene. Strain relaxation on GaN is gradual. © *2015 AIP Publishing LLC*. [http://dx.doi.org/10.1063/1.4929697]

Topological surface(interface) state represents a novel quantum state of matter, which has attracted a lot of research attention lately for interests in fundamental science as well as practical applications.[1–5] Bi_2Se_3 is a representative three-dimensional (3D) topological insulator (TI) having the rhombohedral crystal structure ($R\bar{3}m$).[6,7] The crystal of Bi_2Se_3 consists of stacks of quintuple layers (QLs) of chemically bonded Se-Bi-Se-Bi-Se and is held by the van der Waals (vdW) forces. Such a structural and bonding property of Bi_2Se_3 leads to some unique growth properties that are characteristics of the vdW epitaxy.[8,9]

Originating from the different topological electronic structures of matter,[1,10] topological state will reside in a narrow region at the interface between a TI and an ordinary insulator (OI) or vacuum. The crystal quality of this interface(surface) region is then crucial for the experimental investigation of the topological properties. When a TI is deposited on a substrate of an OI, two interfaces are created: the top TI/vacuum interface (i.e., the surface) and the bottom TI/substrate interface. Topological states exist on both and transport studies of such films inevitably reflect both interfaces. Often the bottom interface is of a poorer quality and so knowledge of the deposit-substrate interface is crucial to fully account the experimental data.

In this letter, we report a reflection high-energy electron diffraction (RHEED) study of initial stage Bi_2Se_3 growth by molecular-beam epitaxy (MBE) on two different substrates: GaN and graphene. Supplemented by scanning tunneling microscopy (STM), we observe distinctly different growth behaviors of Bi_2Se_3 on these two substrates. While the epifilm is highly textured on GaN with an initial residual strain of $\sim$3%, it is strain-free and of a better quality on graphene. This finding improves the current understanding of strain in epitaxial Bi_2Se_3 layers.[11,12] As strain in a TI can effectively modify the topological states,[13–15] an experimental study of strain in TI is fundamentally interesting and practically important for application purposes.

Bi_2Se_3 was deposited in a customized Omicron MBE reactor[16] from elemental Bismuth (Bi) and Selenium (Se) sources in the Knudsen cells. The cell temperature of the Bi source was 500 °C and that of Se was at 110 °C. For the latter, the orifice was heated at 210 °C by a second set of filaments to prevent Se condensation. The flux ratio between Bi and Se was 1:10 and the film growth rate was 0.2 QLs/min according to post-growth film thickness measurements by cross-sectional transmission electron microscopy. The substrate temperature was 200 °C throughout. Ga-face GaN substrate was thermally treated in ultrahigh vacuum (UHV) until a clean (1×1) pattern emerged in the RHEED. Multilayer graphene was prepared by heating Si-face 4H-SiC wafer at $\geq$1200 °C following the procedure documented in the literature.[17,18] During Bi_2Se_3 deposition, the sample surface was constantly monitored by the RHEED operated at 10 keV. The diffraction patterns on the phosphorus screen were captured by a high-speed CCD camera (AVT Stingray F046B) and the intensity data were acquired by a 1394 card and processed by a desktop computer. The spacing D between diffraction streaks was extracted by locating the intensity peak positions of the line profiles across the first-order $(0\bar{1})$ and (01) streaks through computer fitting. The lattice constant of the deposit, a_{sample}, was derived from D by the formula

$$\frac{a_{sample}}{a_{ref}} = \frac{D_{ref}}{D_{sample}}, \tag{1}$$

where a_{ref} refers to the (in-plane) lattice constant of a reference film, e.g., the substrate. D_{sample} and D_{ref} are the measured inter-diffraction streak spacing of the deposit and the

a)E-mail: mhxie@hku.hk

This article is copyrighted as indicated in the article. Reuse of AIP content is subject to the terms at: http://scitation.aip.org/termsconditions. Downloaded to IP: 147.8.230.149 On: Wed, 23 Sep 2015 02:28:28

reference material (substrate), respectively, reflecting the reciprocal lattice constants of the corresponding materials. STM measurements of the grown films were carried out in an adjacent UHV chamber using an Omicron STM facility at room-temperature (RT). For all measurements, the constant current mode was used. The tunneling current and sample bias were 0.1 nA and 1.0 V, respectively. To enhance features of surface steps and defects, differential images obtained by digitally differentiating the intensity over space coordinates were also presented besides the topographic images.

On GaN, growth of Bi_2Se_3 proceeds by formation of an initial polycrystalline layer followed by gradual crystallization upon increasing deposit thickness. Figs. 1(a)–1(c) present the RHEED patterns of a sample during initial stage deposition on GaN. One observes that the streaky pattern of the smooth GaN surface [Fig. 1(a)] changes quickly to a ring pattern superimposed with streaks corresponding to Bi_2Se_3 at about 1 QL [Fig. 1(b)]. The ring pattern then recedes gradually and gives way to streaks again with increasing film thickness [Fig. 1(c)]. The ring pattern signifies a polycrystalline nucleation layer of Bi_2Se_3 at the beginning, which can be caused by the huge chemical and structural differences between Bi_2Se_3 and GaN. A polycrystalline film may also be instigated by the low diffusivity of adatoms on GaN, for which adatom-substrate interaction is expectedly strong due to possible chemical bonding. Nuclei of Bi_2Se_3 can be strained by the constraint of the substrate lattice. The strained Bi_2Se_3 nuclei or crystallites are likely distorted and twisted and their coalescence will produce a polycrystalline layer. The coexistence in Fig. 1(b) of the streaky and ring patterns, on the other hand, suggests both "epitaxial" Bi_2Se_3 domains (where the *c*-axis of Bi_2Se_3 aligns with the surface normal of GaN(0001)) and randomly oriented crystallites to coexist. The receding ring pattern accompanied by the enhancement of the streaky pattern with increasing deposition thickness [Fig. 1(c)] implies the improvement of the film quality with thickness.

We note that even for very thick films, they remain highly "in-plane" textured. Changing the azimuthal angle of the RHEED shows little change of the diffraction patterns except for small intensity variations. The sample must thus contain randomly oriented domains in the "in-plane" directions despite that they are well aligned in the "out-of-plane" (i.e., the *c*-axis) direction for thick layers. The texturing of epitaxial Bi_2Se_3 on GaN is best revealed in the low-energy electron diffraction (LEED) pattern shown in Fig. 1(d), in which a circular ring rather than diffraction spots are observed despite the slight variation in intensity along the ring. The latter implies some preferred in-plane crystallographic orientations to exist, which becomes clearer and more pronounced if one adopts the so called "two-step" deposition process as pointed out in an early publication.[16]

The improvement of crystal quality of Bi_2Se_3-on-GaN with increasing film thickness, from the initial polycrystalline to finally an in-plane textured film, may be understood by considering the anisotropic growth rates of Bi_2Se_3 crystal faces. Given a small crystallite, the *c*-plane, which is of the vdW surface, has no dangling bond and thus the lowest surface energy. On the contrary, the other faces inclined to the *c*-plane have high energies. As the crystallite develops, the low-energy surface will grow at the expense of the high-energy planes. Kinetically, atoms adsorbed on the *c*-face diffuse faster and can always reach the "edges" where they become incorporated in crystal. So, a crystallite will grow predominantly sideways, leading to the enlargement of the *c*-face. If a crystallite has its *c*-plane parallel to the substrate surface, it receives the largest amount of the deposit atoms from the flux and so grows faster. For those where their *c*-faces are inclined to the substrate surface, they receive fewer atoms from the flux and thus grow slower. Ultimately, crystallites with their *c*-planes parallel to GaN(0001) prevail and the epifilm becomes aligned along the *c*-axis out of the initially randomly oriented crystallites in the nucleation layer. This kinetics can be characteristic of growth of other layered materials where the *c*-plane is always the growing surface even if the substrate is not of the low-index surface.[19,20] In-plane lattice alignment of the epifilm, on the other hand, has to be driven by other factors such as the energy potentials of the vdW interface. The latter is generally a weaker effect in vdW epitaxy, so heeling of in-plane texturing can be a much slower process.

On graphene, Bi_2Se_3 growth follows a much simpler process, which does not go through the initial polycrystalline stage. Figs. 2(a)–2(c) record the evolution of the RHEED patterns during Bi_2Se_3 deposition on multilayer graphene formed by heating SiC. As seen, upon the commencement of Bi_2Se_3 deposition, streaky RHEED patterns corresponding to a strain-free Bi_2Se_3 emerge in the background of the graphene pattern [Fig. 2(b)]. After about 1 QL growth, only the Bi_2Se_3 pattern becomes visible. Unlike that on GaN, Bi_2Se_3 on graphene is not very textured. In-plane alignment of $[10\bar{1}0]_{Bi_2Se_3} \parallel [10\bar{1}0]_{Graphene}$ is identified, though 30° rotation domains are also present as revealed in the RHEED and

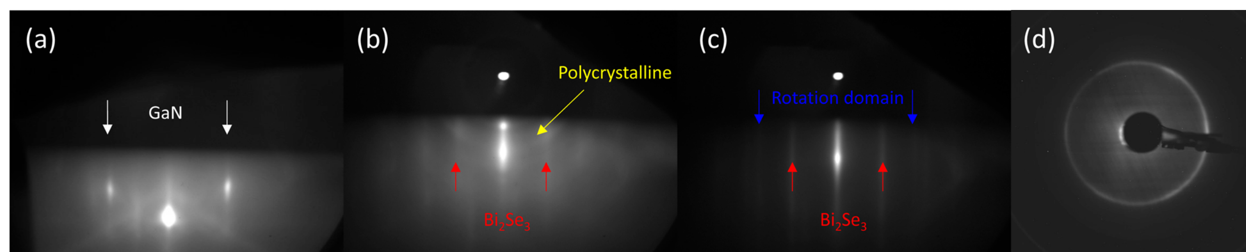

FIG. 1. (a)–(c) RHEED patterns of, respectively, the substrate (GaN), ∼1 QL and 40 QLs of Bi_2Se_3 surfaces. (d) LEED pattern of the 40 QLs Bi_2Se_3 grown on GaN. The vertical arrows in (a)–(c) mark the 1st-order diffraction streaks of the substrate or epitaxial Bi_2Se_3. The inclined yellow arrow points at the polycrystalline ring.

This article is copyrighted as indicated in the article. Reuse of AIP content is subject to the terms at: http://scitation.aip.org/termsconditions. Downloaded to IP: 147.8.230.149 On: Wed, 23 Sep 2015 02:28:28

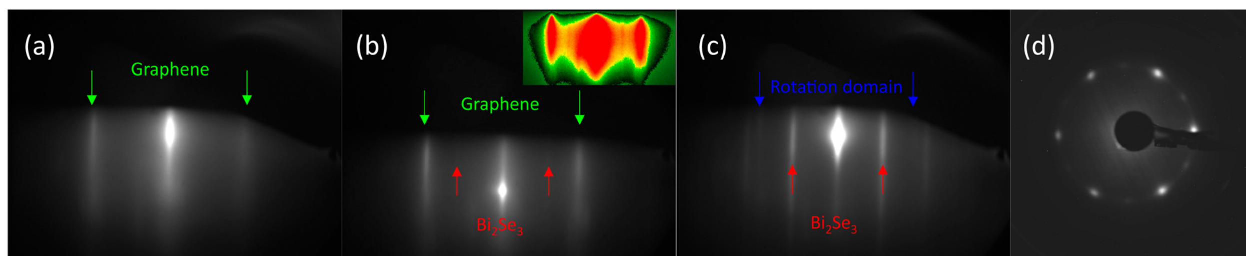

FIG. 2. (a)–(c) RHEED patterns of, respectively, the substrate (graphene/SiC), ~1 QL and 40 QLs of Bi_2Se_3 surfaces. (d) LEED pattern of the 40 QLs Bi_2Se_3 film grown on graphene. The vertical arrows in (a)–(c) mark the 1st-order diffraction streaks of the substrate or epitaxial Bi_2Se_3. The inset in (b) is a "heat map" of (b) to enhance the pattern and shows diffraction streaks of Bi_2Se_3.

LEED [Figs. 2(c) and 2(d)]. In the LEED, instead of the circular ring, spotty patterns are observed, signaling the in-plane alignment of the crystal lattice of Bi_2Se_3.

Graphene is a vdW substrate, on which there is no dangling bond. Deposit-substrate interaction is expectedly weak. As will be shown later, epitaxial Bi_2Se_3 is strain-free on graphene from the very beginning, contrasting that on GaN where a tensile strain is recorded. Unstrained Bi_2Se_3 nuclei on graphene substrate have their lattices undistorted and untwisted, coalescence of which would naturally result in a better film. Because there is no strain, the surface potential expectedly becomes more prominent in affecting and guiding the deposit for the aligned epitaxial relations, which represents an important feature of the vdW epitaxy.[8,9]

Fig. 3 presents STM topographic [(a) and (c)] and derivative [(b) and (d)] images of the Bi_2Se_3 films grown on GaN [(a), (b)] and graphene [(c), (d)] for the same thickness of 40 QLs. The corresponding RHEED patterns of these films resemble that of Figs. 1(c) and 2(c), respectively. From the topographic images of Figs. 3(a) and 3(c), one observes that both films are terminated mainly by the *c*-plane terraces delineated by single or multiple QL steps. For the film grown on GaN [Fig. 3(a)], one also notes multiple steps emerging from the flat terraces, indicating bunches of screw dislocations or boundaries of twisted domains in the film.[21] On the differential image of Fig. 3(b), these large steps appear like the faults in geology. This feature is in accord with the RHEED observation that in-plane texturing remains upon continuous growth of the film. In other words, even if the top-film appears globally aligned with the *c*-axis, local misalignments retain and manifest by domain boundaries or bunch of the screw dislocations. On graphene, on the other hand, one sees large triangular islands or mounds [Fig. 3(c)]. Importantly, few multi-QL high steps are seen from the flat terraces. Instead, one observes single QL steps (e.g., pointed by the black arrow in Fig. 3(d)) that emerge from the flat terraces and manifest as spirals, signaling growth at single and isolated screw dislocations,[22] or the specific step pinning mechanism of the step-growth.[23] The latter film is obviously less twisted or tilted, consistent with the early RHEED observations.

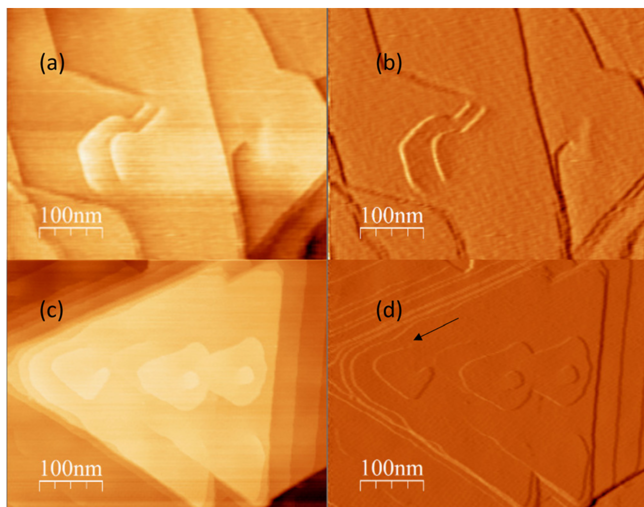

FIG. 3. (a) STM image of 40 QLs Bi_2Se_3 deposited on GaN. (b) Derivative image of (a). (c) STM image of 40 QLs Bi_2Se_3 grown on graphene. (d) Derivative image of (c).

Having discussed the structural and morphological properties of epitaxial Bi_2Se_3 on GaN versus graphene, we now shift our attention to the lattice constant and strain evolution during initial stage Bi_2Se_3 deposition on the two substrates. Figs. 4(a) and 4(b) depict film thickness (or deposition time) dependence of the in-plane lattice constant (a) of the deposits as derived by Eq. (1) from the measured inter-streak spacing D of the RHEED. As is seen, on graphene (red curve), epitaxial Bi_2Se_3 is strain-free from the very beginning, whereas on GaN (black curve), it is $\varepsilon \sim 3\%$ tensile strained for the initially deposited Bi_2Se_3 layer. Here, strain ε is defined as $\varepsilon = (a - a_0)/a_0$, where a_0 refers to the lattice constant of strain-free Bi_2Se_3, and a is derived from Eq. (1). The tensile strain relaxes gradually to the bulk crystal lattice constant with increasing thickness on GaN. We remark that the ~3% strain measured by the RHEED is significant, well above the resolution limit (~0.3%) of our RHEED measurement estimated by statistical analyses and by experimental observation of the lattice constant variation with temperature.

Epitaxial growth of Bi_2Se_3 on graphene represents an example of the vdW epitaxy, where deposit-substrate interaction is weak at the interface. An unstrained epifilm is therefore expected. The fact that the (in-plane) lattice constant of sub-QL Bi_2Se_3 on graphene is the same as that of the bulk crystal suggests that single QL clusters or islands has the same equilibrium lattice constant as the bulk crystal. This appears inconsistent with a recent report of an intrinsically enlarged lattice constant of ultrathin Bi_2Se_3 layer grown on Si,[11] reflecting possibly a substrate effect. The observed lattice stretching of Bi_2Se_3 on GaN can, on the other hand, be attributed to the constraint of the substrate lattice due to a strong heterointerface interaction. As noted earlier, although textured, the deposited Bi_2Se_3 on GaN still

This article is copyrighted as indicated in the article. Reuse of AIP content is subject to the terms at: http://scitation.aip.org/termsconditions. Downloaded to IP: 147.8.230.149 On: Wed, 23 Sep 2015 02:28:28

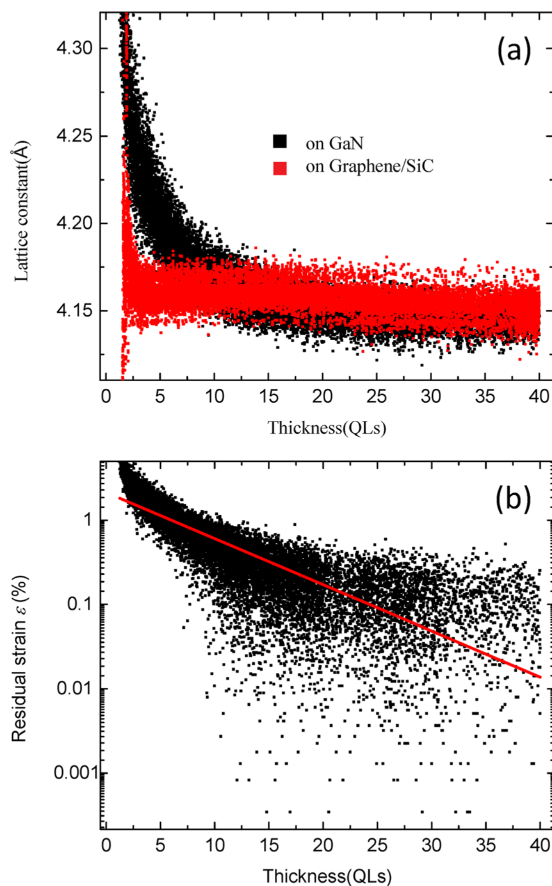

FIG. 4. (a) In-plane lattice constants of epitaxial Bi_2Se_3 on GaN (black) and graphene (red) plotted as a function of deposit thickness. (b) Strain in epitaxial Bi_2Se_3 grown on GaN presented in semi-logarithm plot. The red line represents the least-square fitting by a simple exponential function.

shows a tendency of crystallographic alignment, i.e., and $[0001]_{Bi_2Se_3} \parallel [0001]_{GaN}$ and $[10\bar{1}0]_{Bi_2Se_3} \parallel [10\bar{1}0]_{GaN}$. For such an aligned epitaxial relation, the lattice misfit amounts to $\sim$30%, too large to be sustained by the epifilm. However, we note that there is a "magic match" between GaN and Bi_2Se_3 lattices when epitaxial Bi_2Se_3 is tensile-strained at $\sim$2.7%, i.e., $4a_{GaN} = 3\tilde{a}_{Bi_2Se_3}$, where $\tilde{a}_{Bi_2Se_3} \approx 4.25$ Å is the strained Bi_2Se_3 lattice constant. This is in good agreement with the RHEED measurements. Past studies have suggested that Bi_2Se_3 can grow readily on various substrates, many of which do not have the magic lattice matching with Bi_2Se_3 and some even do not have the right symmetry. It is, therefore, quite tolerant for Bi_2Se_3 epitaxy along the c-axis direction. Nevertheless, there are few data with regard to the strain in Bi_2Se_3 epilayers at the very initial stage of deposition. Instead, strain-free (thick) films were widely reported in the literature. Our observation of the tensile strain in epitaxial Bi_2Se_3 on GaN but no strain on graphene may thus reflect the role of interface interaction on Bi_2Se_3 nucleation and growth. When Bi_2Se_3 film grows thicker ($\geq$2 QLs), the weak vdW interaction in between Bi_2Se_3 QLs makes strain relaxation to readily occur. The result of Fig. 4 reveals, however, a nonexponential strain relaxation process [*cf.* Fig. 4(b)].[24] If we insist on an exponential fit [the red line in Fig. 4(b)], a characteristic length of about 4 QLs is derived.

In summary, we have followed the initial stage Bi_2Se_3 deposition on two very different substrates, GaN and graphene, and revealed distinct growth properties and the strain states of the epifilms. While it is tensile-strained on GaN, epitaxial Bi_2Se_3 is strain-free from the beginning on graphene. Accompanied with this is the difference in morphology and the crystallinity of the epifilms, which is better on graphene substrate. These differences may be accounted for by the different interaction strengths between the deposit and the substrate. The above results may be extended to other vdW versus covalent substrates. Manipulating strain in a TI film is attractive for tuning the topological states, which is thus of great fundamental and practical interests for further studies.

The work described in this paper was supported in full from a grant of the SRFDP and RGC ERG Joint Research Scheme of Hong Kong RGC and the Ministry of Education of China (Grant No. M-HKU709/12).

[1] C. L. Kane and E. J. Mele, Phys. Rev. Lett. **95**, 146802 (2005).
[2] M. Z. Hasan and C. L. Kane, Rev. Mod. Phys. **82**, 3045 (2010).
[3] X.-L. Qi and S.-C. Zhang, Phys. Today **63**(1), 33 (2010).
[4] B. H. Yan and S. C. Zhang, Rep. Prog. Phys. **75**, 096501 (2012).
[5] C.-Z. Chang, J. Zhang, X. Feng, J. Shen, Z. Zhang, M. Guo, K. Li, Y. Ou, P. Wei, L.-L. Wang, Z.-Q. Ji, Y. Feng, S. Ji, X. Chen, J. Jia, X. Dai, Z. Fang, S.-C. Zhang, K. He, Y. Wang, L. Lu, X.-C. Ma, and Q.-K. Xue, Science **340**, 167 (2013).
[6] H. J. Zhang, C.-X. X. Liu, X.-L. L. Qi, X. Dai, Z. Fang, and S.-C. C. Zhang, Nat. Phys. **5**, 438 (2009).
[7] Y. Xia, D. Qian, D. Hsieh, L. Wray, A. Pal, H. Lin, A. Bansil, D. Grauer, Y. S. Hor, R. J. Cava, and M. Z. Hasan, Nat. Phys. **5**, 398 (2009).
[8] A. Koma, Thin Solid Films **216**, 72 (1992).
[9] S. Z. Butler, S. M. Hollen, L. Cao, Y. Cui, J. A. Gupta, H. R. Gutiérrez, T. F. Heinz, S. S. Hong, J. Huang, A. F. Ismach, E. Johnston-Halperin, M. Kuno, V. V. Plashnitsa, R. D. Robinson, R. S. Ruoff, S. Salahuddin, J. Shan, L. Shi, M. G. Spencer, M. Terrones, W. Windl, and J. E. Goldberger, ACS Nano **7**, 2898 (2013).
[10] L. Fu and C. Kane, Phys. Rev. B **76**, 045302 (2007).
[11] M. Vyshnepolsky, C. Klein, F. Klasing, A. Hanisch-Blicharski, and M. Horn-von Hoegen, Appl. Phys. Lett. **103**, 111909 (2013).
[12] M. Eddrief, P. Atkinson, V. Etgens, and B. Jusserand, Nanotechnology **25**, 245701 (2014).
[13] W. Liu, X. Peng, C. Tang, L. Sun, K. Zhang, and J. Zhong, Phys. Rev. B **84**, 245105 (2011).
[14] S. M. Young, S. Chowdhury, E. J. Walter, E. J. Mele, C. L. Kane, and A. M. Rappe, Phys. Rev. B **84**, 85106 (2011).
[15] Y. Liu, Y. Y. Li, S. Rajput, D. Gilks, L. Lari, P. L. Galindo, M. Weinert, V. K. Lazarov, and L. Li, Nat. Phys. **10**, 294–299 (2014).
[16] H. D. Li, Z. Y. Wang, X. Kan, X. Guo, H. T. He, J. N. Wang, T. L. Wong, N. Wang, M. H. Xie, Z. Y. Wang, J. N. Wang, T. L. Wong, N. Wang, and M. H. Xie, New J. Phys. **12**, 103038 (2010).
[17] I. Forbeaux, J.-M. Themlin, and J.-M. Debever, Phys. Rev. B **58**, 16396 (1998).
[18] T. Ohta, A. Bostwick, T. Seyller, K. Horn, and E. Rotenberg, Science **313**, 951 (2006).
[19] Y. Takagaki, B. Jenichen, and J. Tominaga, Phys. Rev. B **87**, 245302 (2013).
[20] X. Liu, D. J. Smith, J. Fan, Y.-H. Zhang, H. Cao, Y. P. Chen, J. Leiner, B. J. Kirby, M. Dobrowolska, and J. K. Furdyna, Appl. Phys. Lett. **99**, 171903 (2011).
[21] A. Zhuang, J.-J. Li, Y.-C. Wang, X. Wen, Y. Lin, B. Xiang, X. Wang, and J. Zeng, Angew. Chem., Int. Ed. Engl. **53**, 6425 (2014).
[22] W. K. Burton, N. Cabrera, and F. C. Frank, Philos. Trans. R. Soc., A **243**, 299 (1951).
[23] Y. Liu, M. Weinert, and L. Li, Phys. Rev. Lett. **108**, 115501 (2012).
[24] J. Y. Tsao, *Materials Fundamentals of Molecular Beam Epitaxy* (Elsevier, 1993), p. 151.

This article is copyrighted as indicated in the article. Reuse of AIP content is subject to the terms at: http://scitation.aip.org/termsconditions. Downloaded to IP: 147.8.230.149 On: Wed, 23 Sep 2015 02:28:28